Crystal Growth

Deutsche Ausgabe: DOI: 10.1002/ange.201504416
Internationale Ausgabe: DOI: 10.1002/anie.201504416

A Family of Molecular Sieves Containing Framework-Bound Organic Structure-Directing Agents

*Jun Kyu Lee, Jiho Shin, Nak Ho Ahn, Alessandro Turrina, Min Bum Park, Youngchul Byun, Sung June Cho, Paul A. Wright, and Suk Bong Hong**

Abstract: *Organic structure-directing agents (OSDAs), such as quaternary ammonium cations and amines, used in the synthesis of zeolites and related crystalline microporous oxides usually end up entrapped inside the void spaces of the crystallized inorganic host lattice. But none of them is known to form direct chemical bonds to the framework of these industrially important catalysts and adsorbents. We demonstrate that ECR-40, currently regarded as a typical silicoaluminophosphate molecular sieve, constitutes instead a new family of inorganic-organic hybrid networks in which the OSDAs are covalently bonded to the inorganic framework. ECR-40 crystallization begins with the formation of an Al–OSDA complex in the liquid phase in which the Al is octahedrally coordinated. This unit is incorporated in the crystallizing ECR-40. Subsequent removal of framework-bound OSDAs generates Al-O-Al linkages in a fully tetrahedrally coordinated framework.*

The synthesis of inorganic-organic hybrid molecular sieves with organic moieties incorporated into the porous inorganic framework is of great interest[1] because it is one effective way of utilizing the organic functionality as a new catalytic and/or adsorption site, as well as of modifying the internal surface selectivity of zeolitic materials with three-dimensional (3D) frameworks made up of four-connected networks of atoms (Si, Al, P, Ga, Ge, etc.) bridged by oxygen atoms. The strategies developed to date, in the search for such hybrid solids, involve either the direct synthesis using organosilanes containing organic functional groups as a (partial) silica source and alkylammonium-bound organosilanes as structure-directing agents,[2] or the post-synthetic treatment using similar organosilane species as pillaring or silylating agents.[3] Thus, they rely on the use of organic species which already contain an atom susceptible of incorporation as a tetrahedral atom (T-atom) in the zeolitic framework.

The synthesis of ECR-40, first reported as a silicoaluminophosphate (SAPO) molecular sieve with the MEI topology in 1999, includes the use of either tris(2-hydroxyethyl)methylammonium ($THMA^+$) or bis(2-hydroxyethyl)dimethylammonium ($BHDMA^+$) ions as organic structure-directing agents (OSDAs).[4] Our interest in this material began with the unexpected gauche conformation of (2-hydroxyethyl)trimethylammonium ($HTMA^+$) ions within as-made UZM-22, an MEI-type aluminosilicate zeolite,[5] stabilized by one intramolecular hydrogen bond between the oxygen atom of its OH group and the hydrogens of carbon atoms linked to the charged nitrogen center.[6] Like $HTMA^+$, both $THMA^+$ and $BHDMA^+$ contain polar OH groups which can participate not only in intramolecular C–H···O hydrogen bonding, but also in intermolecular hydrogen bonding to the other OSDA molecules or to the molecular sieve framework. Moreover, ECR-40 was deemed to be isostructural with ZSM-18, the type material for MEI, containing odd-membered rings, such as 5-rings, which are usually absent in tetrahedral aluminophosphate-based frameworks[7] because of Loewenstein's rule, that is, the avoidance of tetrahedral Al-O-Al linkages.[8]

^{13}C magic angle spinning nuclear magnetic resonance (MAS NMR) spectroscopy shows, by the presence of broadened resonances, that the OSDA molecules within as-made ECR-40 synthesized with $THMA^+$, designated ECR-40A herein, are much less mobile than the same organic cations exchanged into calcined UZM-22 (see Figure S1 in the Supporting Information). This data prompted us to solve the structure of as-made ECR-40A using synchrotron powder X-ray diffraction (XRD) and Rietveld analysis. As for ZSM-18,[9] the XRD pattern obtained was successfully indexed as hexagonal ($a = 13.1860$ Å, $c = 16.1086$ Å). We extracted individual reflection intensities from the pattern to a minimum d-spacing of 1.0 Å using a LeBail algorithm, assuming the space group $P6_3$, and then attempted to obtain an initial structure of as-made ECR-40A using two different dual-space methods, that is, the FOCUS algorithm[10] and the powder charge flipping (pCF) algorithm combined with the histogram matching procedure (see Figure S2 and Tables S1–S3).[11]

The zeolite-specific program, FOCUS, found the MEI framework as a suitable model structure for as-made ECR-40A. However, the electron density map generated with the pCF algorithm reveals that the symmetry of specific T-atoms was broken. Moreover, there are additional electron density peaks within the 12-ring channel (see Figure S3), and they are indicative of the ordering of the OSDAs occluded. This finding led us to refine the model structure using both

[*] J. K. Lee, Dr. J. Shin, N. H. Ahn, Dr. M. B. Park, Dr. Y. Byun, Prof. S. B. Hong
Center for Ordered Nanoporous Materials Synthesis
School of Environmental Science and Engineering
POSTECH, Pohang 790-784 (Korea)
E-mail: sbhong@postech.ac.kr
Homepage: http://zeolites.postech.ac.kr
A. Turrina, Prof. P. A. Wright
EaStCHEM School of Chemistry
University of St. Andrews, St. Andrews, KY16 9ST (UK)
Prof. S. J. Cho
Department of Applied Chemical Engineering
Chonnam National University, Gwangju 500-757 (Korea)

Supporting information for this article is available on the WWW under http://dx.doi.org/10.1002/anie.201504416.

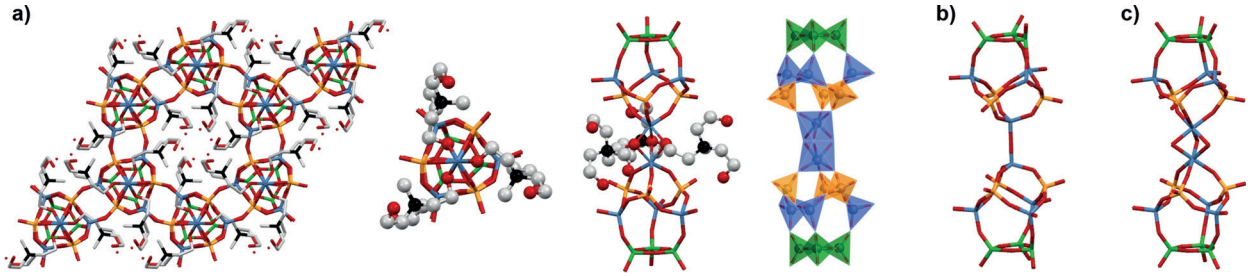

Figure 1. Crystal structures of ECR-40A. a) Top view (far left) of the 12-ring channel in the as-made, hydrated form of ECR-40A with an organic content of ca. 30 wt%, according to a combination of elemental and thermal analyses. Top (second from left) and side (second from right) views of its structural building unit. The $THMA^+$ ions covalently bonded to the framework Al atoms are indicated with a ball-and-stick model, and the water oxygen atoms are represented with dots. The structural unit is also displayed as a combination of TO_4 tetrahedra and AlO_6 octahedra (right). $THMA^+$ ions are omitted for clarity. Side views of the building unit in the calcined, dehydrated (b) and rehydrated (c) forms of ECR-40A. Al blue, P orange, Si green, O red, C gray, N black. Hydrogen atoms are omitted for clarity.

algorithms for the high-angle X-ray reflections with $d \leq 3.0$ Å. The final refined structure reveals that an oxygen atom in one of the three OH groups of each $THMA^+$ ion is within covalent distance (1.93 and 2.03 Å) to framework Al atoms located along the *c* axis at a distance of 2.84 Å apart (Figure 1a). Hence, these Al atoms are covalently bonded with six oxygen atoms: three O atoms linked to the P atoms and three O atoms in the three OSDA molecules which surround the $[3^14^65^6]$ building unit of the MEI topology.[7] The latter three oxygen atoms are shared by another Al, thus resulting in a pair of face-sharing AlO_6 octahedra (Figure 1a). The existence of abundant AlO_6 octahedra is supported by the appearance of a sharp resonance around −9 ppm in the ^{27}Al multiple-quantum (MQ) MAS NMR spectrum of as-made, dehydrated ECR-40A (see Figure S4). The same result was also observed not only for the OSDA molecules in ECR-40 synthesized with $BHDMA^+$, denoted ECR-40B (see Figure S5 and Tables S4 and S5), but also for those in the other materials prepared in this work (Table 1; see Figures S6 and S7 and Tables S6–S9). Therefore, ECR-40 cannot be considered a traditional molecular sieve any more but a new family of crystalline inorganic-organic hybrid materials, that is, framework-bound OSDA-containing molecular sieves (FOMSs).

Table 1: Representative FOMS synthesis results.[a]

Run	Seeds[b]	$t_{cryst.}$ [days]	R	Product[c] M = Si	M = Ge
1	–	12	THMAOH	ECR-40A	GeAPO-5 + L
2	UZM-22	12	THMAOH	ECR-40A	L + (PST-10A)
3	ECR-40A	12	THMAOH	ECR-40A	PST-10A
4	–	24	BHDMAOH	PB + L	PB
5	UZM-22	12	BHDMAOH	ECR-40B	L + (PST-10B)
6	ECR-40A	12	BHDMAOH	ECR-40B	PST-10B
7	–	24	HTMAOH	PB + L	PB
8	UZM-22	16	HTMAOH	ECR-40C[d]	L + PST-10C
9	ECR-40A	16	HTMAOH	ECR-40C + PB	PST-10C
10	–	24	BHMA	ECR-40D + SAPO-34	PB
11	UZM-22	12	BHMA	ECR-40D	PB
12	ECR-40A	12	BHMA	ECR-40D	PST-10D + PB + (GeAPO-34)
13	–	24	BHEA	L + SAPO-34 + PB	PB
14	UZM-22	12	BHEA	ECR-40E	PB
15	ECR-40A	12	BHEA	ECR-40E	L + PST-10E + PB
16	–	36	TPMAOH	PB	PB
17	UZM-22	36	TPMAOH	PB	PB
18	ECR-40A	36	TPMAOH	PB	PB
19	–	36	THAOH	L + PB	L + PB
20	UZM-22	36	THAOH	L + PB	L + PB
21	ECR-40A	36	THAOH	L + PB	L + PB

[a] The composition of the synthesis mixture was $2.0\,R{\cdot}1.0\,Al_2O_3{\cdot}0.75\,P_2O_5{\cdot}0.75\,MO_2{\cdot}80\,H_2O$. SAPO and GeAPO FOMS syntheses were performed under rotation (60 rpm) at 160 °C and 140 °C, respectively, unless otherwise stated. [b] If required, 2 wt% (of the alumina in the synthesis mixture) of either as-made UZM-22 or ECR-40A crystals were added as seeds. [c] The product appearing first is the major phase, and that obtained in a trace amount is given in parentheses. L and PB are layered phase and pseudoboehmite, respectively, the alumina starting material. [d] Performed at 140 °C.

To our knowledge, there are two already known FOMSs: one is the gallophosphate (GaPO) material synthesized using 1,4,8,11-tetraazacyclotetradecane (Cyclam) as an OSDA in an HF-pyridine nonaqueous solvent system and the other is the germanate SU-77, crystallized with ethylenediamine in fluoride media.[12] Regardless of the very poor structural stability, however, both Cyclam-GAPO and SU-77 are substantially different from the FOMSs reported here in that their inorganic parts are not truly zeolite 3D (4,2)-nets. For example, the former material contains framework pentacoordinated Ga atoms with Ga–F bonds, as well as hexacoordinated Ga species in which four of the coordinated sites are bonded to the four nitrogen atoms from Cyclam, while the other two are bonded to oxygen atoms from PO_4 tetrahedra.[12a]

We also solved the structures of the calcined, dehydrated and rehydrated forms of ECR-40A (Figure 1b,c; see Fig-

ure S8 and Tables S10–S13). All framework atoms in calcined, dehydrated ECR-40A are completely tetrahedrally coordinated, which can be further evidenced by ^{27}Al MQMAS and ^{31}P MAS NMR experiments (see Figures S4 and S9), and are characterized by the MEI topology. As previously reported,[4b] there are extensive violations of Loewenstein's rule,[8] which in materials crystallized under hydrothermal conditions, similar to those employed here, are considered unstable. The violations observed in calcined, dehydrated ECR-40A are intrinsically structural, but not occasional, because all face-sharing AlO_6 octahedra are transformed into corner-sharing AlO_4 tetrahedra upon $THMA^+$ removal (Figure 1b). By contrast, the structure of calcined, rehydrated ECR-40A shows that the two adjacent Al atoms at site T_4 are octahedrally coordinated with three water oxygen atoms once again (Figure 1c). This finding indicates that the Al-O-Al linkages in calcined, dehydrated ECR-40A are not stable enough to stand rehydration. When exposed to ambient air after recalcination at 550 °C, in fact, the material becomes amorphous.

When $THMA^+$ was replaced with the equivalent amount of tripropylmethylammonium ($TPMA^+$), which has no OH groups but is similar in molecular size and shape to $THMA^+$, the solid isolated even after 36 days at 160 °C continued to be pseudoboehmite (PB), the alumina starting material, regardless of the presence of 2 wt % (of the alumina in the SAPO gel) of either as-made UZM-22 or ECR-40A crystals which were added as seeds. When using $HTMA^+$, bis(2-hydroxyethyl)methylamine (BH-MA), and bis(2-hydroxyethyl)ethylamine (BHEA) as an OSDA, on the other hand, we were able to crystallize three new members of the ECR-40 family (Table 1; see Figure S10 and Table S14), but seeding is essential for their crystallization. This result indicates that the presence of OH groups in OSDAs is a critical factor governing the crystallization of ECR-40-type FOMSs. Since the use of tetrakis(2-hydroxyethyl)ammonium (THA^+) always gave a mixture of a layered phase and PB, however, there appears to be an optimum degree of hydrophilicity of OSDAs to facilitate FOMS crystallization. We also found that their germanoaluminophosphate (GeAPO) version, termed the PST-10 family, can be synthesized by substituting germanium oxide for colloidal silica in the synthesis mixture, although seeding is again necessary to crystallize their pure form. Therefore, the compositional regime of FOMSs is likely to be considerably wide.

To investigate the crystallization mechanism of this new class of inorganic-organic hybrid materials, we separated the mother liquors and solid products at different times during the $THMA^+$-mediated synthesis of ECR-40A and measured their multinuclear solution and solid-state NMR spectra, respectively. When the crystallization was performed under rotation (60 rpm) at 160 °C, it was complete after 12 days (Figure 2a). While the most prominent ^{27}Al NMR resonance

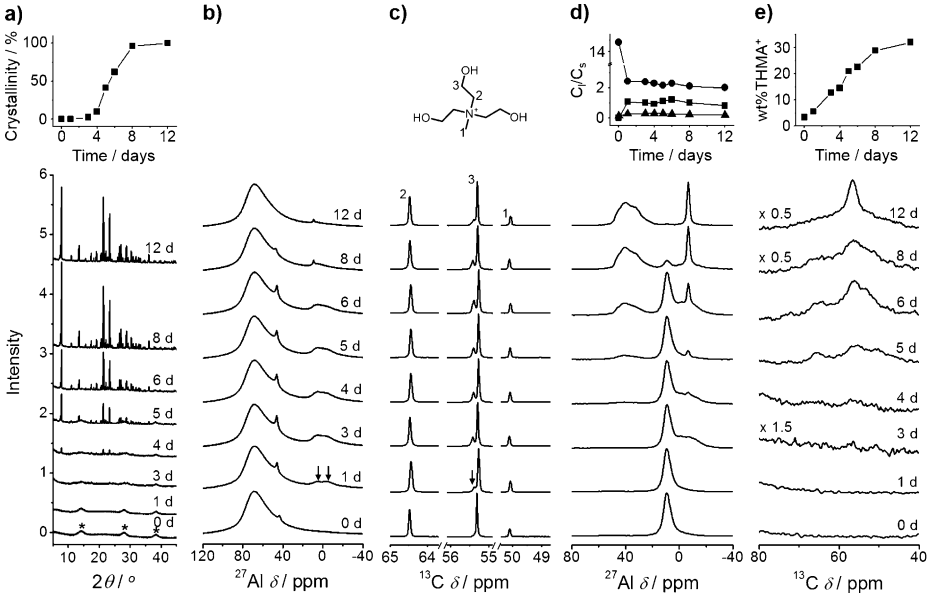

Figure 2. Characterization of a series of mother liquors and solid products separated after ECR-40A crystallization at 160 °C at different times. a) Powder XRD patterns and d) ^{27}Al and e) ^{13}C MAS NMR spectra of solid product series. The X-ray peaks from pseudoboehmite, the alumina starting material, are marked by asterisks. To more clearly display changes in the resonance intensity, the amount of solid samples used in the MAS NMR experiments was kept constant. The relative crystallinities of solid products, the concentration ratios of Al (squares), P (circles), and Si (triangles) in mother liquors to the corresponding elements in solid products, and the organic contents of solid product series are also shown in (a), (d), and (e), respectively. b) ^{27}Al and c) ^{13}C NMR spectra of mother liquor series. Two octahedral ^{27}Al resonances around $\delta = 5$ and -4 ppm and one ^{13}C resonance at $\delta = 55.4$ ppm assignable to the CH_2 carbon atoms bonded to the OH group in $THMA^+$ are indicated with arrows. The assignment of each ^{13}C resonance from $THMA^+$ is also shown in (c).

around $\delta = 68$ ppm in unheated solution may be assigned to the $Al(OH)_4^-$ species bonded to HPO_4^{2-} ions,[13] the formation of octahedral Al species after 1 day is established by two additional weak resonances around $\delta = 5$ and -4 ppm (Figure 2b). The ^{13}C NMR spectrum of this mother liquor gives a new weak resonance at $\delta = 55.4$ ppm, which should correspond to the methylene carbon atom next to the OH group in $THMA^+$ bonded to Al (Figure 2c).

The new ^{27}Al and ^{13}C resonances become stronger for up to about 5 days at 160 °C, when the characteristic X-ray reflections from ECR-40A are clearly visible, but become weaker as crystallization proceeds (Figure 2a–c). This change implies that at the early stage of ECR-40A synthesis the Al-$THMA^+$ complexes in solution are consumed to build the

framework. We also found that almost all silica in the synthesis mixture remains in the solid phase during the crystallization process (Figure 2d), which can be further supported by the ^{29}Si NMR results (see Figure S11). Notably, the ^{27}Al MAS NMR spectrum of the solid product recovered after 3 days gives a new resonance around $\delta = -7$ ppm, thus corresponding to octahedral Al (Figure 2d). Moreover, the ^{13}C and ^{29}Si MAS NMR spectra of this product show signs of the THMA$^+$ resonances with strongly restricted mobility (Figure 2e), and a resonance around $\delta = -94$ ppm, which is assignable to the Si_3(2Si,2Al) species (see Figure S11),[4b] if all Si atoms in this solid are assumed to locate at site T_3 in the ideal MEI framework, respectively. These new resonances become stronger until complete crystallization occurs.

The characterization results allow us to propose a reliable mechanism for ECR-40A crystallization (Figure 3). First, an Al-THMA$^+$ complex, comprising two octahedral Al atoms bridged by three THMA$^+$ ions, is formed by the reaction of two Al atoms bonded to HPO_4^{2-} with three THMA$^+$ ions in the liquid phase. The solution ^{27}Al and ^{13}C NMR spectra (Figure 2b,c) of the mother liquor collected after 1 day at 160 °C, as well as the crystal structure of as-made ECR-40A (Figure 1a), support the presence of covalent bonds between the Al and THMA$^+$ oxygen atoms in this complex.[14] It is worth noting that Al-THMA$^+$ formation, as well as ECR-40A synthesis, is highly sensitive to the pH of the starting SAPO gel (see Figure S12 and Table S15). The Al-THMA$^+$ complex is then incorporated within the solid phase, the oxide composition of which is identical with that of the inorganic part of as-made ECR-40A (Figure 2d). Hence, the next logical step would be the formation of the inorganic-organic building unit of ECR-40A containing 3-rings (Figure 1a).[4b] Finally, the formation and growth of ECR-40A nuclei take place in a self-assembled manner similar to that observed for zeolite crystallization. However, the overall crystallization mechanism of ECR-40A is substantially different from that of typical conventional porous solids such as zeolite molecular sieves and metal–organic frameworks.[15] This mechanism also allows us to understand the formation of Al pairs which become tetrahedral Al-O-Al linkages within its OSDA-free form (i.e., calcined ECR-40A).

The N_2 sorption experiments on the FOMSs synthesized here reveal that all of them show negligible uptakes at 1 bar and 25 °C. However, a CO_2 uptake of 0.3 mmol g^{-1} at the same pressure and temperature was observed for as-made ECR-40A, synthesized using THMA$^+$ with three ethanol groups. Also, a considerably larger CO_2 uptake (1.0 mmol g^{-1}) was obtained from as-made ECR-40D prepared using BHMA, which has two ethanol groups and is thus somewhat smaller than THMA$^+$ (see Figure S13). Given the wide diversity of the type of zeolite structure building units,[7] as well as of OSDAs, we believe that the synthesis of FOMSs with larger zeolitic microporosities and different inorganic framework structures and pendant organic moieties in the pores may be possible, if tailored judiciously, and will provide invaluable opportunities not only for extending our knowledge of many important aspects of the synthesis, structures, and modification of ordered microporous materials, but also for creating new applications.

In summary, we have reported the discovery of molecular sieves containing framework-bound OSDAs and a plausible formation pathway for this novel class of inorganic-organic hybrid crystals. ECR-40 crystallization begins with the formation of an Al-OSDA complex in the liquid phase. The "structural" making of tetrahedral Al-O-Al linkages upon removal of framework-bound OSDAs in such hybrid materials is possible thanks to the octahedral nature of the Al-OSDA complex initially formed.

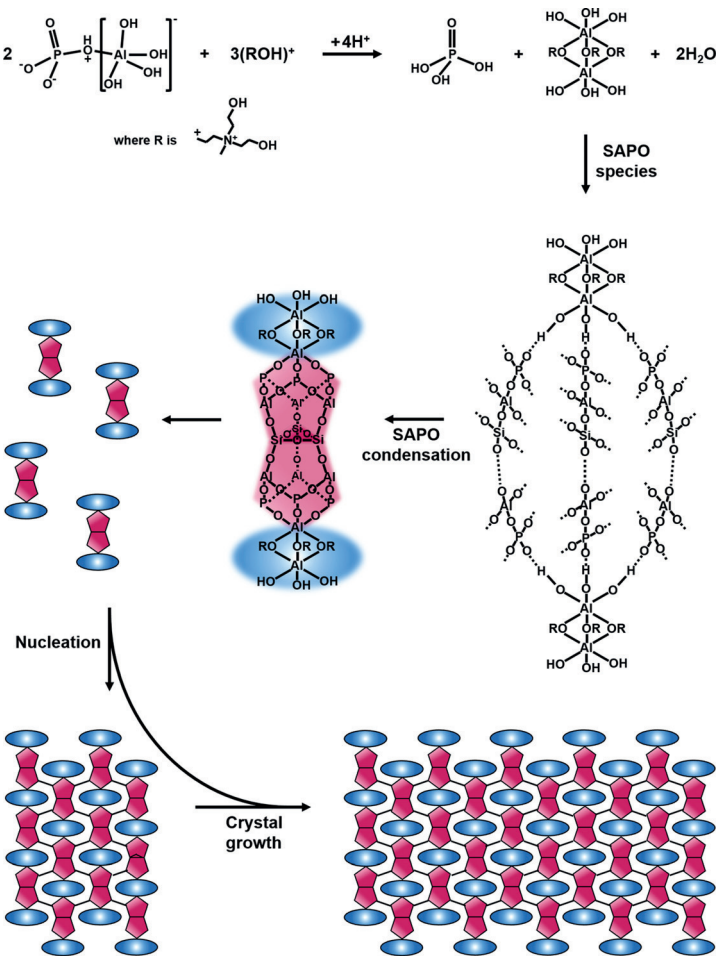

Figure 3. Schematic illustration of a plausible formation pathway for ECR-40A crystals in the presence of THMA$^+$ ions as an OSDA.

Acknowledgements

This work was supported by the NCRI (2012R1A3A-2048833) and BK 21-plus programs through the National Research Foundation of Korea. We thank J. H. Lee for technical assistance, C. Fernandez for ^{27}Al MQMAS NMR experiments, P. A. Cox for helpful discussion, and PAL for synchrotron diffraction beam time. PAL is supported by MSIP and POSTECH.

Keywords: crystal growth · materials science · organic–inorganic hybrid composites · structure elucidation · X-ray diffraction

How to cite: *Angew. Chem. Int. Ed.* **2015**, *54*, 11097–11101
Angew. Chem. **2015**, *127*, 11249–11253

[1] C. W. Jones, *Science* **2003**, *300*, 439–440.
[2] a) C. W. Jones, K. Tsuji, M. E. Davis, *Nature* **1998**, *393*, 52–54; b) K. Yamamoto, Y. Sakata, Y. Nohara, Y. Takahashi, T. Tatsumi, *Science* **2003**, *300*, 470–472; c) H.-X. Li, M. A. Camblor, M. E. Davis, *Microporous Mater.* **1994**, *3*, 117–121; d) G. Bellussi, A. Carati, E. D. Paola, R. Millini, W. O. Parker, Jr., C. Rizzo, S. Zanardi, *Microporous Mesoporous Mater.* **2008**, *113*, 252–260; e) G. Bellussi, et al., *Angew. Chem. Int. Ed.* **2012**, *51*, 666–669; *Angew. Chem.* **2012**, *124*, 690–693.
[3] a) U. Díaz, Á. Cantín, A. Corma, *Chem. Mater.* **2007**, *19*, 3686–3693; b) P. Wu, J. Ruan, L. Wang, L. Wu, Y. Wang, Y. Liu, W. Fan, M. He, O. Terasaki, T. Tatsumi, *J. Am. Chem. Soc.* **2008**, *130*, 8178–8187; c) H. Gies, et al., *Chem. Mater.* **2012**, *24*, 1536–1545.
[4] a) D. E. W. Vaughan, US Pat 5976491, **1999**; b) M. Afeworki, D. L. Dorset, G. J. Kennedy, K. G. Strohmaier, *Stud. Surf. Sci. Catal.* **2004**, *154*, 1274–1281.
[5] M. A. Miller, J. G. Moscoso, S. C. Koster, M. G. Gatter, G. J. Lewis, *Stud. Surf. Sci. Catal.* **2007**, *170*, 347–354.
[6] M. B. Park, S. J. Cho, S. B. Hong, *J. Am. Chem. Soc.* **2011**, *133*, 1917–1934.
[7] C. Baerlocher, L. B. McCusker, Database of Zeolite Structures: http://www.iza-structure.org/databases/.
[8] W. Loewenstein, *Am. Mineral.* **1954**, *39*, 92–96.
[9] S. L. Lawton, W. J. Rohrbaugh, *Science* **1990**, *247*, 1319–1321.
[10] R. W. Grosse-Kunstleve, L. B. McCusker, C. Baerlocher, *J. Appl. Crystallogr.* **1999**, *32*, 536–542.
[11] C. Baerlocher, L. B. McCusker, L. Palatinus, *Z. Kristallogr.* **2007**, *222*, 47–53.
[12] a) D. S. Wragg, G. B. Hix, R. E. Morris, *J. Am. Chem. Soc.* **1998**, *120*, 6822–6823; b) L. Fang, L. Liu, Y. Yun, A. K. Inge, W. Wan, X. Zou, F. Gao, *Cryst. Growth Des.* **2014**, *14*, 5072–5078.
[13] R. F. Mortlock, A. T. Bell, C. J. Radke, *J. Phys. Chem.* **1993**, *97*, 775–782.
[14] G. Scott, R. W. Thompson, A. G. Dixon, A. Sacco, Jr., *Zeolites* **1990**, *10*, 44–50.
[15] a) C. S. Cundy, P. A. Cox, *Microporous Mesoporous Mater.* **2005**, *82*, 1–78; b) N. Stock, S. Biswas, *Chem. Rev.* **2012**, *112*, 933–969.

Received: May 15, 2015
Published online: August 5, 2015

